International Journal for Housing Science and Its Applications
Publish August 10, 2025. Volume 46, Issue 4 Pages 6503-6513

https://doi.org/10.70517/ijhsa464552

Variable-Step Size Complex Total Maximum Versoria Criterion Algorithm for Robust DOA Estimation Under Impulsive Noise

Kequan Zhu[1,*] and Qiying Sun[1]
[1] School of Communications and Information Engineering, Nanjing University of Posts and Telecommunications, Nanjing, Jiangsu, 210023, China
Corresponding authors: (e-mail: 13878120210@163.com).

Abstract Low-complexity adaptive filtering-based direction of arrival (DOA) estimation algorithms have been proposed to avoid the computationally expensive steps of covariance matrix estimation and eigenvalue decomposition (EVD). However, their performance degrades significantly in impulsive noise scenarios. To address this issue, an adaptive filtering algorithm named complex total maximum versoria criterion (CTMVC) algorithm has been designed to perform robust DOA estimation under impulsive noise. Nonetheless, determining an appropriate step size remains challenging, yet it plays a vital role in accurate DOA estimation. This paper puts forward a variable step-size scheme for the CTMVC algorithm by incorporating cumulative gradient error and signal power estimation, thereby striking a compromise between the speed of convergence and the error of the steady-state. Furthermore, this article provides a detailed computational complexity analysis of the proposed algorithm. Extensive simulations across various metrics highlight the enhanced effectiveness of the VSS-CTMVC over current algorithms.

Index Terms Direction Of Arrival (DOA) Estimation, Variable-Step Size, Maximum Versoria Criterion, Impulsive Noise, Adaptive Filtering

I. Introduction

Direction of arrival (DOA) estimation holds vital applications within radar detection, sonar positioning, wireless communication, and antenna systems [1], [2]. Among existing methods, power scanning based on beamforming remains widely adopted for its intuitiveness and ease of implementation, though its resolution is fundamentally constrained by the Rayleigh limit [3]. To realize super-resolution in DOA estimation and resolve the Rayleigh resolution limit, numerous solutions have been proposed by researchers [4], [5]. Among these, eigenvalue decomposition (EVD)-based algorithms are the most widely recognized, including the estimation of signal parameters via rotational invariance techniques (ESPRIT), the multiple signal classification (MUSIC) algorithm, and their respective variants [6], [7]. MUSIC and its variants leverage EVD of the covariance matrix of the signal received by array to distinguish between the subspaces of noise and signal, exploiting the orthogonality between the noise subspaces and the direction vectors of the source signals for high-precision spectral peak searches [8]. However, the inherent computational complexity of EVD impedes real-time DOA estimation on hardware platforms. Moreover, when the search step size is very small, the computational cost of spectral peak searching becomes significantly large. Although the ESPRIT algorithm does not require spectral peak searching to obtain estimated DOAs, its implementation still relies on EVD, retaining significant computational burdens.

To avoid the processes of EVD and the computation of covariance matrix, and to achieve a DOA estimation algorithm of low-complexity, the fixed-step-size least mean square (FSS-LMS) algorithm is proposed as an adaptive filtering algorithm based on the minimum mean square error (MSE) criterion to obtain weights orthogonal to the direction vectors of the source signals, thereby obtaining the spatial spectrum [9]. Nevertheless, its fixed step size compromises adaptability to signal-to-noise ratio (SNR) variations, forcing a trade-off between steady-state error and convergence speed. To address this issue, the variable-step-size LMS (VSS-LMS) algorithm is proposed, which adaptively adjusts the step size to provide better estimation performance [10]. Conventionally, these adaptive filtering-based DOA estimators assign the first element of array as the reference element while others as auxiliary sensors. However, the signal received at the reference sensor inherently contains noise, introducing estimation bias that neither FSS-LMS nor VSS-LMS resolves. To address the limitation, several adaptive filtering DOA estimation algorithms that consider bias compensation have been proposed [11], such as the variable-step size gradient descent total least squares (VSS-GDTLS) algorithm [12].

However, the above algorithms are derived under the assumption of Gaussian noise, and they experience significant performance degradation under impulsive noise. To counter this challenge, the complex total least mean m-estimation (CTLMM) algorithm was introduced to enhance robust DOA estimation under impulsive noise, though

its effectiveness is limited by the order of the filter [13]. Beyond m-estimation, the maximum versoria criterion (MVC) function exhibits strong noise resilience. This motivated the complex total MVC (CTMVC) algorithm for DOA estimation under impulse noise with input noise and bias compensation [14]. Since the step size of CTMVC algorithm must be set to adapt to SNR variations, it faces a critical practical challenge, SNR cannot be known a priori in complex real-world environments, making optimal step size selection fundamentally problematic.

To resolve this issue, this paper designs a variable-step size scheme driven by the cumulative gradient error and the estimated signal power. Subsequently a robust DOA estimation algorithm, named VSS-CTMVC, is proposed in this paper. A high-resolution spatial spectrum is achieved by taking the reciprocal of the array pattern, where the spectral peaks reflect the estimated DOAs. Moreover, this study conducts a detailed analysis of computational complexity. Simulations across diverse metrics confirm that the proposed VSS-CTMVC algorithm significantly surpasses existing adaptive filtering-based DOA algorithms in impulse noise scenarios.

Notation: $|\cdot|$ represents the modulus of a complex number or the absolute value of a real number, $\|\cdot\|$ signifies the L2 norm, $\mathrm{E}(\cdot)$ represents the operator of expectation, $(\cdot)^*$ denotes the complex conjugate, $[\cdot]^H$ and $[\cdot]^T$ respectively symbolize conjugate transposition and transposition.

II. Signal model

According to Figure 1, the uniform linear array (ULA) is constructed from M omnidirectional antenna elements spaced by half of the signal wavelength. The steering vector of array $\boldsymbol{a}(\theta_l) \in \mathbb{C}^{M\times 1}$ is defined as

$$\boldsymbol{a}(\theta_l)=\left[1, e^{-j\pi\sin(\theta_l)},\ldots, e^{-j(M-1)\pi\sin(\theta_l)}\right]^T \tag{1}$$

Suppose that $L(L<M)$ statistically independent and narrowband signals impinge on the ULA from the far field in directions $\theta_0,\theta_1,\ldots,\theta_{L-1}$, and K snapshots are collected. The received signal $\boldsymbol{x}(k) \in \mathbb{C}^{M\times 1}$ during the kth snapshot is expressed as

$$\boldsymbol{x}(k)=\sum_{l=0}^{L-1} s_l(k)\boldsymbol{a}(\theta_l)+\boldsymbol{n}(k)=\boldsymbol{z}(k)+\boldsymbol{n}(k) \tag{2}$$

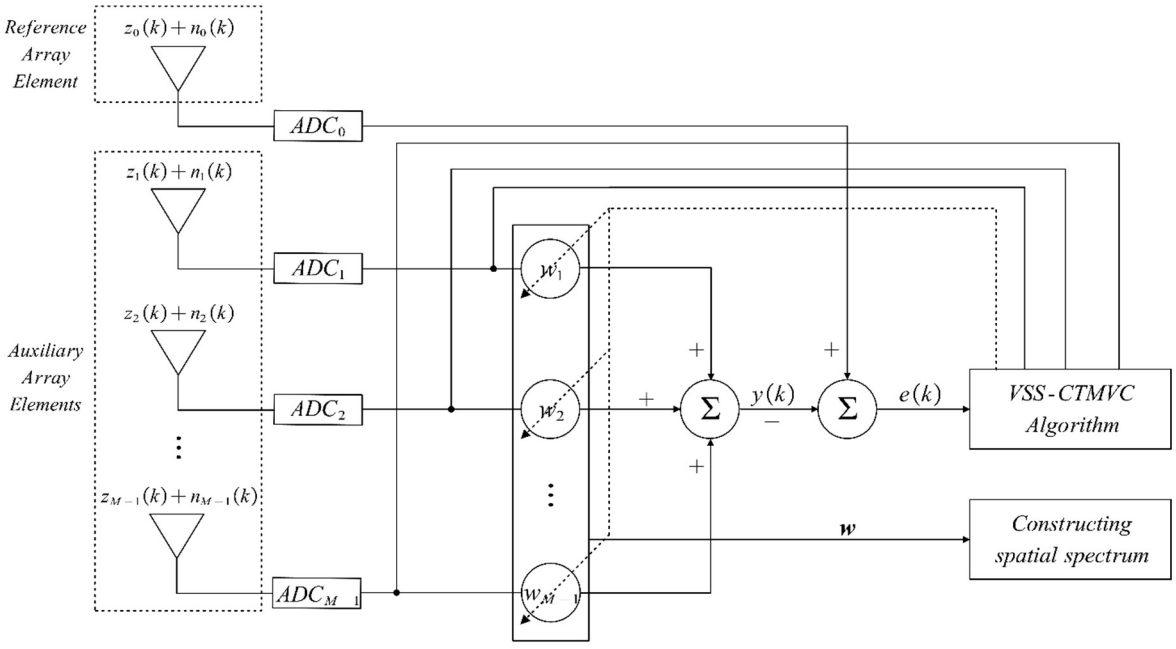

Figure 1: Adaptive nulling antenna array for DOA estimation

where $s_l(k)$ denotes the lth vector of source signal, $\boldsymbol{z}(k)=\left[z_0(k), z_1(k),\ldots, z_{M-1}(k)\right]^T \in \mathbb{C}^{M\times 1}$ and $\boldsymbol{n}(k)=\left[n_0(k), n_1(k),\ldots, n_{M-1}(k)\right]^T \in \mathbb{C}^{M\times 1}$ respectively signify the noise-free signal and noise received at ULA.

Let the first sensor element as the reference element and the remaining elements as the auxiliary array elements. As depicted in Figure 2, the received signals of the reference element $x_0(k)$ and the elements of auxiliary array $\dot{\boldsymbol{x}}(k) \in \mathbb{C}^{(M-1)\times 1}$ are formulated respectively as

$$x_0(k) = \sum_{l=0}^{L-1} s_l(k) + n_0(k) = z_0(k) + n_0(k) \tag{3}$$

$$\dot{\boldsymbol{x}}(k) = \sum_{l=0}^{L-1} s_l(k)\dot{\boldsymbol{a}}(\theta_l) + \dot{\boldsymbol{n}}(k) = \dot{\boldsymbol{z}}(k) + \dot{\boldsymbol{n}}(k) \tag{4}$$

where $n_0(k)$ and $z_0(k)$ stand for the noise and noise-free signal received at the reference element, while $\dot{\boldsymbol{n}}(k) = \left[n_1(k), n_2(k), \ldots, n_{M-1}(k)\right]^T$ and $\dot{\boldsymbol{z}}(k) = \left[z_1(k), z_2(k), \ldots, z_{M-1}(k)\right]^T \in \mathbb{C}^{(M-1)\times 1}$ stand for the noise and noise-free signal received by the elements of auxiliary array, $\dot{\boldsymbol{a}}(\theta_l) = \left[e^{-j\pi\sin(\theta_l)}, \ldots, e^{-j(M-1)\pi\sin(\theta_l)}\right]^T \in \mathbb{C}^{(M-1)\times 1}$ defines the vector of steering associated with the elements of auxiliary array.

The instantaneous error signal $e(k)$ of adaptive filter in this paper takes the form of [15]

$$e(k) = x_0(k) - \boldsymbol{w}^H(k)\dot{\boldsymbol{x}}(k) = x_0(k) - y(k) \tag{5}$$

where $y(k) = \boldsymbol{w}^H(k)\dot{\boldsymbol{x}}(k)$ represents the output signal of adaptive filter as well as $\boldsymbol{w}(k) = \left[w_1(k), w_2(k), \ldots, w_{M-1}(k)\right]^T \in \mathbb{C}^{(M-1)\times 1}$ refers to the adaptive filter weight vector [16].

As shown in Figure 2, the objective is to adjust the weights $\boldsymbol{w}(k)$ of the auxiliary elements such that the output of the adaptive filter cancels out with the signal of reference element to create nulls. It is straightforward to observe that, to form nulls in our system, the weight of the reference element needs to be set to 1. Therefore, the overall weight vector for the array is defined as

$$\tilde{\boldsymbol{w}}(k) = \left[1; -\boldsymbol{w}(k)\right] \tag{6}$$

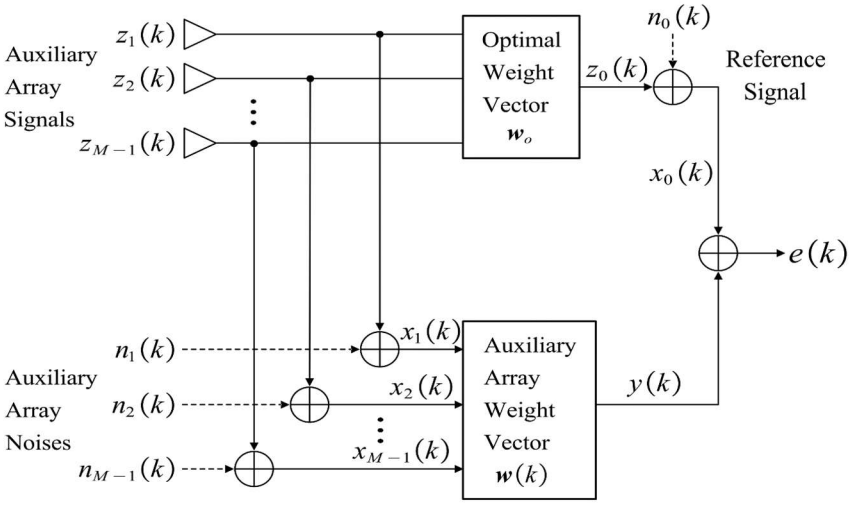

Figure 2: DOA estimation Bias model

Ultimately, the spatial spectrum can be obtained by:

$$P(\theta) = \frac{1}{\left|\tilde{\boldsymbol{w}}^H(k)\dot{\boldsymbol{a}}(\theta)\right|} \tag{7}$$

The angles at which peaks occur in the spatial spectrum serve as estimates of the DOAs of the incoming signals.

III. Proposed variable-step size CTMVC algorithm

III. A. An overview of the CTMVC algorithm

The CTMVC algorithm is motivated by the classical minimum versoria criterion (MVC) and the gradient descent total least squares (GDTLS) method, based on which the corresponding cost function is formulated as:

$$J_{CTMVC}\left[\boldsymbol{w}(k)\right]=\mathrm{E}\left[1\Big/1+\kappa\left(\frac{|e(k)|}{\|\bar{\boldsymbol{w}}\|}\right)^{2}\right] \tag{8}$$

where $\kappa>0$ denotes a related parameter, $\bar{\boldsymbol{w}}(k)=\left[\sqrt{\delta},-\boldsymbol{w}^{H}(k)\right]^{H}$ is an augmented weight vector and $\delta=\sigma_o^{\,2}/\sigma_i^{\,2}$ represents the variance ratio of noise. Consider that the input noise variance is identical across all auxiliary elements. $\sigma_o^{\,2}$ and $\sigma_i^{\,2}$ are corresponding noise variances.

By applying Wirtinger calculus, the gradient of the cost function as shown in Eq. (8) can be derived by:

$$g_{CTMVC}\left(\boldsymbol{w}(k)\right)=\frac{\partial J\left[\boldsymbol{w}(k)\right]}{\partial \boldsymbol{w}^{*}(k)}=\mathrm{E}\left[\frac{\kappa\left[\left(\dot{\boldsymbol{x}}(k)e^{*}(k)\right)\|\bar{\boldsymbol{w}}\|^{2}+\boldsymbol{w}(k)\left(|e(k)|^{2}\right)\right]}{\|\bar{\boldsymbol{w}}\|^{4}+\kappa^{2}\left|e(k)\right|^{4}+2\kappa|e(k)|^{2}\|\bar{\boldsymbol{w}}\|^{2}}\right] \tag{9}$$

The instantaneous gradient vector is given by:

$$\hat{g}_{CTMVC}\left(\boldsymbol{w}(k)\right)=\frac{\kappa\left[\left(\dot{\boldsymbol{x}}(k)e^{*}(k)\right)\|\bar{\boldsymbol{w}}\|^{2}+\boldsymbol{w}(k)\left(|e(k)|^{2}\right)\right]}{\|\bar{\boldsymbol{w}}\|^{4}+\kappa^{2}\left|e(k)\right|^{4}+2\kappa|e(k)|^{2}\|\bar{\boldsymbol{w}}\|^{2}} \tag{10}$$

Based on Eq. (8), the weight vector is updated via stochastic gradient ascent as:

$$\boldsymbol{w}(k+1)=\mu\hat{g}_{CTMVC}\left(\boldsymbol{w}(k)\right)+\boldsymbol{w}(k) \tag{11}$$

where μ denotes the step size.

III. B. Proposed variable step-size mechanism

As observed in the previous review of the CTMVC algorithm, its step size is fixed. However, the appropriate step size required in different environments varies significantly. Therefore, determining a suitable step size is challenging. In this subsection, this paper proposes a scheme that adaptively adjusts the step size to achieve better estimation performance. This scheme is introduced via cumulative gradient error and instantaneous power estimation. Thus, the fixed-step-size μ in Eq. (11) is replaced by a variable-step size $\mu(k)$ described by:

$$\mu(k)=\beta\sigma_x^{\,2}(k)+\eta\left[1\Big/\overline{\xi_g}(k)\right] \tag{12}$$

where $0<\eta<1$ and $0<\beta<\frac{2}{3}$ denotes a small-valued positive control parameter nearly equal to zero. $\sigma_x^{\,2}(k)$ denotes the estimated power of signal explained as:

$$\sigma_x^{\,2}(k)=\frac{1}{\dot{\boldsymbol{x}}^{H}(k)\dot{\boldsymbol{x}}(k)} \tag{13}$$

Here, this article defines $\xi_g(k)$ to be the L2 norm of the vector of instantaneous gradient, which takes the form of:

$$\xi_g(k)=\left\|\hat{g}_{CTMVC}\left(\boldsymbol{w}(k)\right)\right\|=\left\|\frac{\kappa\left[\left(\dot{\boldsymbol{x}}(k)e^{*}(k)\right)\|\bar{\boldsymbol{w}}\|^{2}+\boldsymbol{w}(k)\left(|e(k)|^{2}\right)\right]}{\|\bar{\boldsymbol{w}}\|^{4}+\kappa^{2}\left|e(k)\right|^{4}+2\kappa|e(k)|^{2}\|\bar{\boldsymbol{w}}\|^{2}}\right\| \tag{14}$$

and $\overline{\xi_g}(k)$ is the sum of the cumulative gradient error, which can be computed by:

$$\overline{\xi_g}(k)=\overline{\xi_g}(k-1)+\xi_g(k) \tag{15}$$

To guarantee successful convergence of the proposed algorithm, an upper bound is imposed on $\mu(k)$, defined as:

$$\mu(k)=\begin{cases}\mu_{max}, \mu(k)>\mu_{max}\\ \mu(k), otherwise.\end{cases} \tag{16}$$

To provide a more intuitive presentation of the implementation steps of the proposed VSS-CTMVC algorithm, this paper summarizes these steps within Table 1.

Table 1: Algorithmic steps of VSS-CTMVC

Inputs: $\dot{\boldsymbol{x}}(k)$, $x_0(k)$

Initialization: $\overline{\xi_g}(0)=0$, $\boldsymbol{w}(0)=\boldsymbol{0}$

Parameters: κ, η, β

for $k=1,\ldots,K$

$$y(k)=\boldsymbol{w}^H(k)\dot{\boldsymbol{x}}(k)$$

$$e(k)=x_0(k)-y(k)$$

$$\overline{\boldsymbol{w}}(k)=\left[\sqrt{\delta},-\boldsymbol{w}^H(k)\right]^H$$

$$\hat{g}_{CTMVC}\left(\boldsymbol{w}(k)\right)=\frac{\kappa\left[\left(\dot{\boldsymbol{x}}(k)e^*(k)\right)\|\overline{\boldsymbol{w}}\|^2+\boldsymbol{w}(k)\left(\left|e(k)\right|^2\right)\right]}{\|\overline{\boldsymbol{w}}\|^4+\kappa^2\left|\left|e(k)\right|^4\right|+2\kappa\left|e(k)\right|^2\|\overline{\boldsymbol{w}}\|^2}$$

$$\xi_g(k)=\left\|\hat{g}_{CTMVC}\left(\boldsymbol{w}(k)\right)\right\|$$

$$\overline{\xi_g}(k)=\overline{\xi_g}(k-1)+\xi_g(k)$$

$$\sigma_x^{\,2}(k)=\frac{1}{\dot{\boldsymbol{x}}^H(k)\dot{\boldsymbol{x}}(k)}$$

$$\mu(k)=\beta\sigma_x^{\,2}(k)+\eta\left[1/\overline{\xi_g}(k)\right]$$

$$\mu_{\max}=\frac{2\|\overline{\boldsymbol{w}}(k)\|^2}{\dot{\boldsymbol{x}}^H(k)\dot{\boldsymbol{x}}(k)}$$

$$\mu(k)=\begin{cases}\mu_{max},\mu(k)>\mu_{max}\\ \mu(k),otherwise.\end{cases}$$

$$\boldsymbol{w}(k+1)=\mu\hat{g}_{CTMVC}\left(\boldsymbol{w}(k)\right)+\boldsymbol{w}(k)$$

$$\tilde{\boldsymbol{w}}(k)=\left[1;-\boldsymbol{w}(k)\right]$$

end

$$P(\theta)=\frac{1}{\left|\tilde{\boldsymbol{w}}^H(k)\dot{\boldsymbol{a}}(\theta)\right|}$$

III. C. Analysis of computational complexity

The DOA estimation algorithms computational complexity is typically assessed based on the quantity of complex multiplication operations required [13], which serves as a fundamental criterion in evaluating computational performance. Based on the detailed algorithmic steps of VSS-CTMVC algorithm presented within Table 1, this section analyzes the computational complexity operations of the proposed VSS-CTMVC algorithm and other related algorithms in terms of the number of complex multiplications in this section. The number of complex multiplications required by the proposed algorithm and other comparative algorithms is summarized within Table 2.

Table 2: Comparative Analysis of computational complexity

Algorithm	Complex Multiplications
Proposed	$\mathrm{O}\left(K\left(7M+7\right)+M\psi\right)$
FSS-LMS [9]	$\mathrm{O}\left(K\left(2M-1\right)+M\psi\right)$
VSS-LMS [10]	$\mathrm{O}\left(K\left(3M+3\right)+M\psi\right)$
VSS-GDTLS [12]	$\mathrm{O}\left(K\left(5M+7\right)+M\psi\right)$
CTMVC [13]	$\mathrm{O}\left(K\left(4M+6\right)+M\psi\right)$
MUSIC	$\mathrm{O}\left(M\left(M-L\right)\psi+\left(M-L\right)\psi\right)+\mathrm{O}\left(M^3\right)+\mathrm{O}\left(KM^2\right)$

In Table 2, K represents the number of snapshots, M denotes the number of omnidirectional antenna elements, L stands for the number of narrowband and mutually uncorrelated signals, and ψ is the quantity of scanning angles. For the proposed VSS-CTMVC algorithm, the computational complexity primarily consists of two parts, first, obtaining the weight vector of the filter, which requires $\mathrm{O}\left(K\left(7M+7\right)\right)$, and second, spectral peak searching, which requires $\mathrm{O}\left(M\psi\right)$ and total computational complexity is $\mathrm{O}\left(K\left(7M+7\right)+M\psi\right)$. It is clearly observed that the proposed algorithm exhibits significantly lower computational complexity compared to the MUSIC algorithm, while maintaining slightly higher complexity than other adaptive filter-driven DOA estimation approaches. Furthermore, the proposed algorithm exhibits superior performance relative to existing adaptive estimation methods in DOA estimation, as validated by the simulations presented in the following section.

IV. Results of simulation

Simulation experiments are conducted in this part to evaluate the estimation capability of the VSS-CTMVC and benchmarked against other algorithms. During the simulations, spatial spectrum, root mean square error (RMSE) and resolution probability are employed as three key metrics for evaluating estimation performance. To assess algorithm performance, the spatial spectrum is generated via a random single simulation, whereas the resolution probability and RMSE are computed as the average results across more than 500 independent Monte Carlo simulations. For all considered methods, the angular search interval is uniformly fixed at 0.01 degrees. This fine resolution ensures precise estimation of signal directions while balancing the computational load associated with the search process.

The noise considered in this study is symmetric α-stable (SαS) noise, which is a classical model for simulating environments with strong impulsive interference and can be defined by its characteristic function as [17]:

$$\Gamma\left(k\right)=\exp\left(-\gamma\left|k\right|^{\alpha}\right) \tag{17}$$

where $1\le\alpha\le 2$ describes the impulsive nature of the SαS. Smaller magnitude of α indicates stronger impulsiveness, and it is initialized to 1.4 during the subsequent simulations. $\gamma>0$ acts as a dispersion metric that quantifies how widely the distribution spreads in the vicinity of the origin, similar to the function of variance in the Gaussian noise model. The classical SNR is pointless as the SαS distribution does not possess a second-order moment when α is less than 2. The generalized signal-to-noise ratio (GSNR) extends the traditional definition of SNR to accommodate non-gaussian and impulsive noise environments, which are commonly encountered in practical signal processing applications, thus introducing GSNR described by [18]:

$$\mathrm{GSNR}=10\log_{10}\left\{\mathrm{E}\left[\left|s_l\left(k\right)\right|^2\right]\Big/\gamma_i^{\alpha}\right\} \tag{18}$$

$$\mathrm{GSNR}_{\mathrm{o}}=10\log_{10}\left\{\mathrm{E}\left[\left|s_l\left(k\right)\right|^2\right]\Big/\gamma_o^{\alpha}\right\} \tag{19}$$

where γ_i and γ_o respectively represent the dispersion characteristics associated with the impulsive noise received by the elements of auxiliary array and reference. In our simulations, the configuration parameters for both the comparison algorithms and the proposed algorithm are specified below. κ, η, β of proposed algorithm are fixed at 0.08, 0.9, 0.2, respectively. Within the FSS-LMS algorithm, the step size is configured to $\mu_1=1\times10^{-3}$,the VSS-LMS algorithm are assigned values of $\alpha_1=0.2$, $\gamma_1=2\times10^{-3}$ and $\varepsilon_1=0.2$. The VSS-GDTLS algorithm is implemented with the following parameter settings as $\alpha_2=0.6$, $\chi=5\times10^{-3}$, the CTMVC algorithm are specified as $\kappa_1=0.08$, $\mu_2=0.07$.

IV. A. Spatial spectrum

The spatial spectrum is a fundamental and widely adopted tool for visualizing and analyzing the output behavior of of DOA estimation algorithms. It reflects the signal energy distribution over the angular domain, with distinct peaks indicating the estimated directions of arrival. A well-shaped spectrum with sharp and accurate peaks directly correlates with the resolution and precision of the DOA estimation algorithm.

Figure 3 shows the spatial spectrum of the VSS-CTMVC when processing three impinging signals $\left(0°,30°,35°\right)$ in an impulse noise scenario, as well as the comparison results with VSS-LMS, CTMVC, FSS-LMS, VSS-GDTLS, and MUSIC algorithms. Figure 3 (a) and (b) are obtained when the GSNR is 10 dB along with 15 dB. The number of omnidirectional antenna elements $M=12$, snapshots $K=300$. As indicated in Figure 3 (a), under low GSNR, the proposed algorithm can estimate the correct direction, and the spatial spectrum highest peak relating to the angle of the three impinging signal directions, and the estimation performance is superior to other comparison algorithms. Although the CTMVC algorithm estimation performance is roughly equal to that of the proposed VSS-

CTMVC algorithm, the angle corresponding to the spectrum peak of the VSS-CTMVC algorithm more accurately matches the true arrival angle, and if the step size of CTMVC μ_2 is not adjusted properly, the performance will be greatly reduced. Moreover, when some algorithms have no ability of distinguishing similar signals, VSS-CTMVC can still clearly find out the difference between the two signals and correctly display the corresponding two peaks. Although most algorithms achieve accurate DOA estimation under high GSNR conditions, the proposed algorithm exhibits superior spectral peak concentration at the three impinging directions and effectively distinguishes between the incoming signals. From the spatial spectrum of the two figures, the proposed algorithm has stable estimation performance and can adapt well to different GSNR environments.

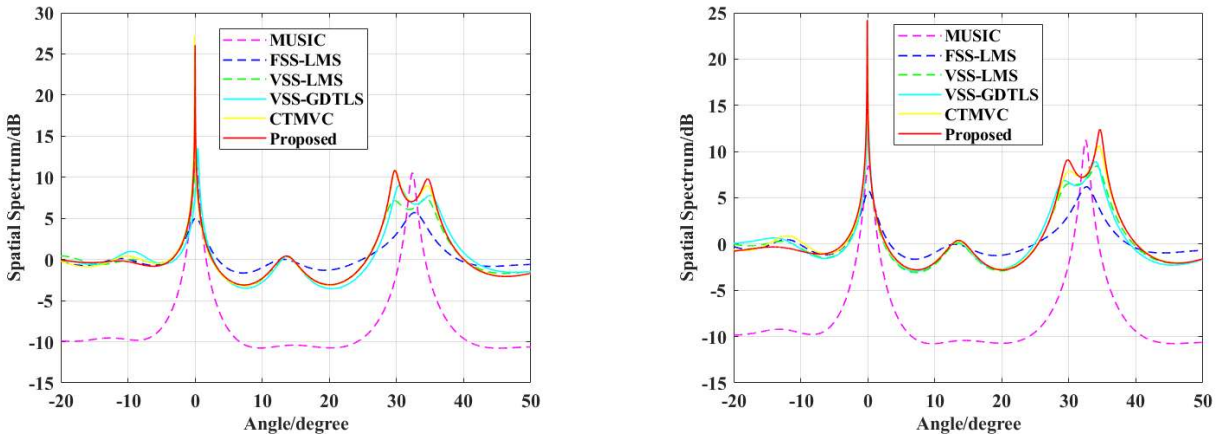

(a) 10 dB GSNR,$\mathrm{GSNR}_{\mathrm{o}}$. (b) 15 dB GSNR,$\mathrm{GSNR}_{\mathrm{o}}$.

Figure 3: RMSE comparisons of various algorithms with 12 antenna elements, 300 snapshots

IV. B. Root mean square error

RMSE is extensively utilized for performance indicator to evaluate the precision of DOA estimations. It measures the average deviation between the estimated directions and the true impinging angles across multiple Monte Carlo trials. A lower RMSE value indicates higher estimation precision and stability of the algorithm.

In this section, the GSNR, number of snapshots K, number of elements M, angle separation $\Delta\theta$ are systematically varied to evaluate the performance of all algorithms under an impulsive noise environment. The corresponding RMSE results are summarized in Figure 4. Specifically, Figures 4 (a)–(c) illustrate the RMSE performance of the VSS-CTMVC and comparison algorithms under impulsive noise, regarding GSNR, number of snapshots, and number of array elements, respectively, when subjected to three impinging signals $(0°,30°,35°)$. RMSE outcomes of various angle separation $\Delta\theta$ with two impinging signals $(30°,30°+\Delta\theta)$ are illustrated in Figure 4 (d). RMSE is formulated as [19]:

$$\mathrm{RMSE}=\sqrt{\frac{1}{LN}\sum_{i=0}^{L-1}\sum_{n=1}^{N}\left|\theta_i-\hat{\theta}_{i,n}\right|^2} \tag{20}$$

where L represents the number of narrowband and mutually uncorrelated signals, N stands for the counts of Monte Carlo experiments, $\hat{\theta}_{i,n}$ and θ_i respectively symbolize the estimated angle of the ith signal during the nth experiment and the real angle of the ith signal. It can be observed from the results that the RMSE of the VSS-CTMVC decreases with increasing GSNR, number of snapshots, angle separation, and consistently outperforms the comparison algorithms. According to Figure 4 (c), the RMSE of the CTMVC algorithm is close to that of the proposed VSS-CTMVC algorithm when $M=16$ or $M=18$, but in general, the RMSE of the VSS-CTMVC is the best. The downward trend of RMSE of the VSS-CTMVC in the above four figures is very reasonable, while the VSS-GDTLS and VSS-LMS in the comparison algorithms are not suitable for the impulse noise environment and show an erroneous trend when $K=400$ shown in Figure 4 (b), which further proves the stability as well as the robustness of the VSS-CTMVC in comparison with other existing algorithms.

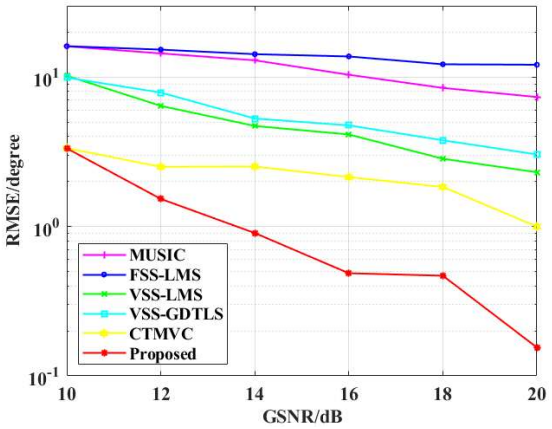

(a) 12 antenna elements, 300 snapshots

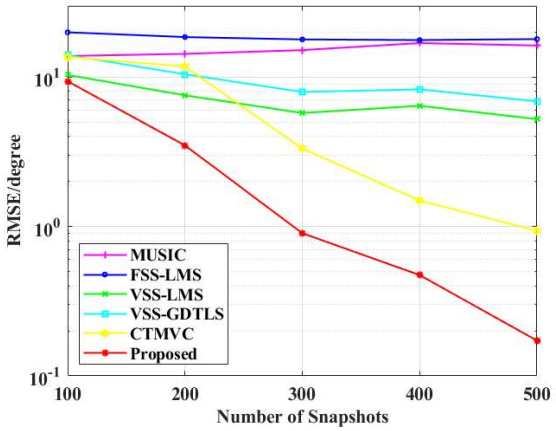

(b) 12 antenna elements, 15 dB GSNR,GSNR_o

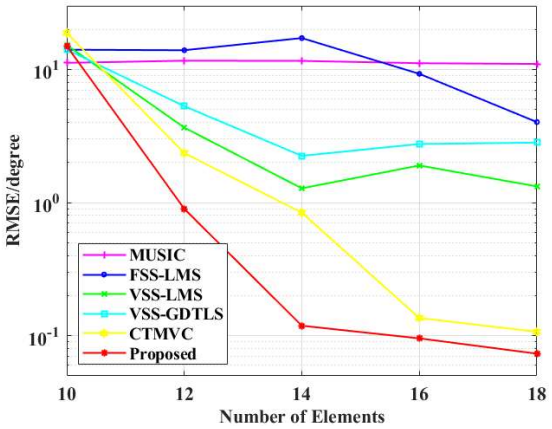

(c) 300 snapshots, 15 dB GSNR,GSNR_o

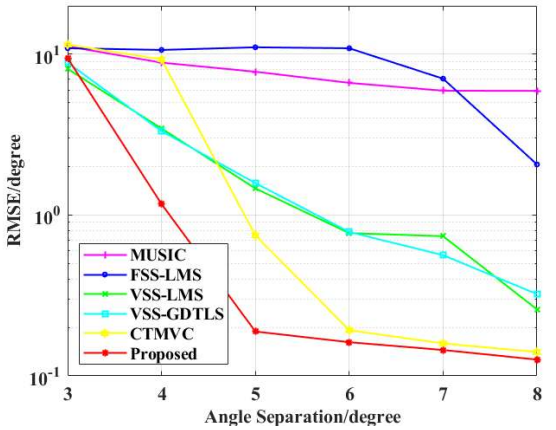

(d) 12 antenna elements, 300 snapshots, 15 dB GSNR,GSNR_o

Figure 4: RMSE comparisons of various algorithms

IV. C. Resolution probability

Resolution probability serves as a key metric for evaluating an ability of algorithm to distinguish between closely spaced signal sources. It quantifies the likelihood that two impinging signals with small angular separation can be correctly resolved by the DOA estimation method. A higher resolution probability indicates better resolvability and angular discrimination performance. In this simulation, the resolution probability is defined as the ratio of successful resolution cases $\sum_{n=1}^{N} \nu\left(\hat{\theta}_{1,n}, \hat{\theta}_{2,n}\right)_n$ over the total counts of Monte Carlo trials. The detailed mathematical formulation of the resolution probability R is given by:

$$R = \sum_{n=1}^{N} \nu\left(\hat{\theta}_{1,n}, \hat{\theta}_{2,n}\right)_n \Big/ N \tag{21}$$

where $\hat{\theta}_{1,n}$ and $\hat{\theta}_{2,n}$ indicate the estimated arrival angles of the first and second signals during the nth experiment, while $\nu\left(\hat{\theta}_{1,n}, \hat{\theta}_{2,n}\right)_n$ corresponds to the function defined as [20]:

$$\nu\left(\hat{\theta}_{1,n},\hat{\theta}_{2,n}\right)_n=\begin{cases}1, & \sqrt{\dfrac{\left(\theta_1-\hat{\theta}_{1,n}\right)^2+\left(\theta_2-\hat{\theta}_{2,n}\right)^2}{2}}<\sqrt{3}\\ 0, & otherwise.\end{cases} \tag{22}$$

where θ_1 and θ_2 represent the angles of two impinging signals, resolution probability $0\le R\le 1$ is used to characterize the resolvability of two signals. When this value is closer to 1, the resolution is higher, and when it is closer to 0, the resolution is lower.

Under impulsive noise conditions and with two impinging signals $(0°,5°)$, the resolution probability outcomes of the VSS-CTMVC and comparison algorithms are presented through Figures 5 (a)–(c), corresponding to varying GSNR, number of snapshots, and number of array elements. The resolution probability outcomes of various angle separation $\Delta\theta$ with two impinging signals $(0°,0°+\Delta\theta)$ are illustrated in Figure 5 (d). The results of simulation show that the VSS-CTMVC resolution probability increases with the growth of GSNR, the number of snapshots, the number of elements, and the increase of angular separation, and it outperforms the comparison algorithm in all cases. Although the algorithm resolution probability of the CTMVC algorithm approaches that of the VSS-CTMVC in some cases, the proposed algorithm still shows strong estimation performance and stability in poor environments (e.g., low GSNR, few snapshots, few elements, and small angular intervals) owing to the variable step size mechanism. This adaptive scheme enables the VSS-CTMVC to dynamically adjust its convergence behavior, thereby maintaining high resolution and robustness.

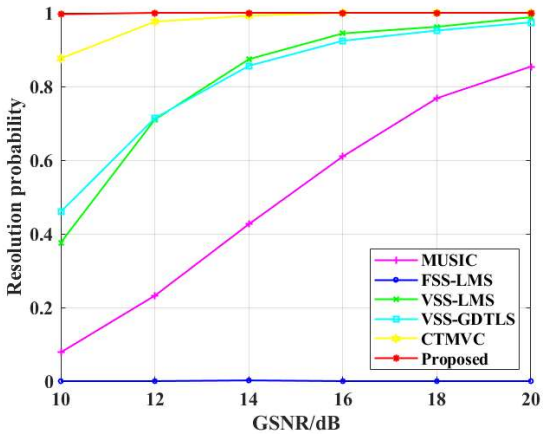

(a) 12 antenna elements, 300 snapshots

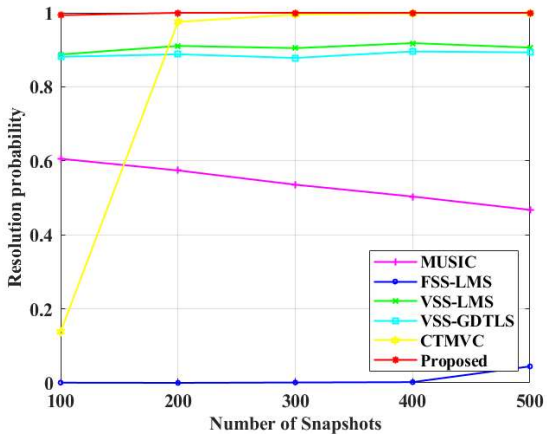

(b) 12 antenna elements, 15 dB GSNR,$GSNR_o$

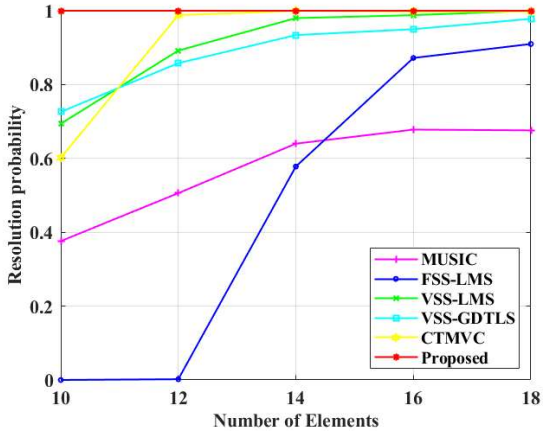

(c) 300 snapshots, 15 dB GSNR,$GSNR_o$

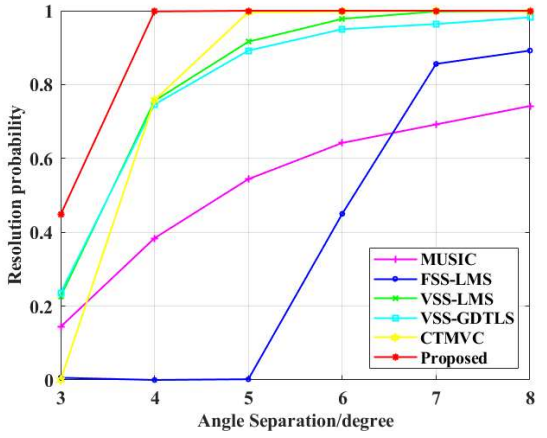

(d) 12 antenna elements, 300 snapshots, 15 dB GSNR,$GSNR_o$

Figure 5: Resolution probability comparisons of various algorithms

V. Conclusion

In this paper, a robust DOA estimation algorithm is proposed, termed VSS-CTMVC, which addresses the limitation of the existing CTMVC algorithm, where the use of a fixed step size hinders the balance between the speed of convergence and the error of steady-state. By introducing a variable step-size scheme that adaptively adjusts the step size based on a combination of cumulative gradient error and power of estimated signal, the proposed algorithm achieves improved adaptability under varying GSNR conditions, thereby enhancing overall DOA estimation performance. The detailed implementation steps of the VSS-CTMVC algorithm are presented, and its computational complexity is analyzed, demonstrating a favorable balance between estimation accuracy and computational efficiency compared to existing methods. To verify the effectiveness of the proposed method, comprehensive simulation experiments are performed under impulsive noise, with comparisons against several comparative algorithms. Performance is evaluated based on the spatial spectrum, RMSE, resolution probability. The results of simulation illustrate that the proposed VSS-CTMVC algorithm significantly outperforms other adaptive filtering-based algorithms under impulsive noise, making it well suited for real-time applications in resource-constrained environments. Future work could explore extending the proposed algorithm to wider application scenarios, further optimizing its computational efficiency, and validating its performance using real-world measured data.

Declaration of Conflicting Interests

The author(s) declared no potential conflicts of interest with respect to the research, author-ship, and/or publication of this article.

Data Sharing Agreement

The datasets used and/or analyzed during the current study are available from the corresponding author on reasonable request.

Funding

The author(s) received no financial support for the research, authorship, and/or publication of this article.

References

[1] Valenti G, Mouhamadou M, Decroze C. Covariance Matrix Reconstruction Based on Regularized Denoising Autoencoders for Direction-of-Arrival Estimation[C]// 2025 IEEE International Radar Conference (RADAR), Atlanta, USA, 2025: 1–6.

[2] Geetha P., Satyasai Jagannath Nanda, Rajendra Prasad Yadav. A Parallel Chaotic Sailfish Optimization Algorithm for Estimation of DOA in Wireless Sensor Array[J]. Physical Communication, 2022, 51: 101536.

[3] Barb G, Otesteanu M, Alexa F, Ghiulai A. Digital Beamforming Techniques for Future Communications Systems[C]// 12th International Symposium on Communication Systems, Networks and Digital Signal Processing (CSNDSP), Porto, Portugal, 2020: 1-4.

[4] Man Yunying, Yang Peng, Yin Lu, et al. An Efficient Multibeamforming Method Based on 1-bit Phase Modulation for Time-Modulated Arrays[J]. IEEE Transactions on Antennas and Propagation, 2025, 73(6): 3654-3665.

[5] Chai Yuqing. Compressed Sensing Based DOA Estimation Algorithm[C]// 2024 IEEE International Symposium on Broadband Multimedia Systems and Broadcasting (BMSB), Toronto, ON, Canada, 2024: 1-5.

[6] Wang Chuanrui, Cui Xiaowei, Liu Gang, et al. Two-Stage Spatial Whitening and Normalized MUSIC for Robust DOA Estimation of GNSS Signals Under Jamming[J]. IEEE Transactions on Aerospace and Electronic Systems, 2025, 61(2): 2557-2572.

[7] Li Jianzhong, Yang Gaolu, Ren Xingqi, et al. Modified ESPRIT and unitary-transformation form for computationally efficient DOA estimation on FPGA[J]. IEEE Transactions on Instrumentation and Measurement, 2025, 74:1-9.

[8] Yin Dayu, Zhang Fei. Uniform Linear Array MIMO Radar Unitary Root MUSIC Angle Estimation[C]// 2020 Chinese Automation Congress (CAC), Shanghai, China, 2020: 578-581.

[9] Zeng Hao, Z. Ahmad, Zhou Jianwen, et al. DOA Estimation Algorithm Based on Adaptive Filtering in Spatial Domain[J]. China Communications, 2016, 13(12): 49-58.

[10] Jalal, Babur, Yang, Xiaopeng, Wu, Xuchen, et al. Efficient Direction-of-Arrival Estimation Method Based on Variable-Step-Size LMS Algorithm[J]. IEEE Antennas and Wireless Propagation Letters, 2019, 18(8): 1576-1580.

[11] S., Joel, Yadav, Shekhar Kumar, et al. Enhanced Bias-Compensated NLMS for Adaptive DOA Estimation[J]. IEEE Sensors Letters, 2024, 8(5): 1-4.

[12] Zhao Haiquan, Luo Wenjing, Liu Yalin, et al. A Variable Step Size Gradient-Descent TLS Algorithm for Efficient DOA Estimation[J]. IEEE Transactions on Circuits and Systems II: Express Briefs, 2022, 69(12): 5144-5148.

[13] Cao Zian, Zhao Haiquan, Liu Yalin, et al. Complex Total Least Mean M-Estimate Adaptive Algorithm for Noisy Input and Impulsive Noise[J]. Circuits, Systems, and Signal Processing, 2024, 43(2): 994-1006.

[14] Zhao Haiquan, Peng Yi, Xu Wenjing. Complex Total Maximum Versoria Criterion Algorithm for DOA Estimation[J]. IEEE Transactions on Circuits and Systems II: Express Briefs, 2024, 71(4): 2489-2493.

[15] Shen Pengcheng, Li Chunguang. Minimum Total Error Entropy Method for Parameter Estimation[J]. IEEE Transactions on Signal Processing, 2015, 63(15): 4079-4090.

[16] S. Leng, W. Ser, C.C. Ko. Adaptive Beamformer Derived from a Constrained Null Steering Design[J]. Signal Processing, 2010, 90(5): 1530-1541.

[17] Zheng Rui, Xu Xu, Ye Zhongfu, et al. Robust Sparse Bayesian Learning for DOA Estimation in Impulsive Noise Environments[J]. Signal Processing, 2020, 171: 107500.

[18] Du Yanan, Wu Hao, Sha Xiang, et al. Robust sparse array-based DOA tracking in impulse noise[C]//Proceedings of the 3rd International Conference on Computing, Communication, Perception and Quantum Technology (CCPQT). Zhuhai, China, 2024:6–10.
[19] Huang Fuyi, Song Fan, Zhang Sheng, et al. Robust Bias-Compensated LMS Algorithm: Design, Performance Analysis and Applications[J]. IEEE Transactions on Vehicular Technology, 2023, 72(10): 13214-13228.
[20] Wagner, Mark, Park, Yongsung, et al. Gridless DOA Estimation and Root-MUSIC for Non-Uniform Linear Arrays[J]. IEEE Transactions on Signal Processing, 2021, 69: 2144-2157.